FINE ALIGNMENT AND WAVEFRONT MAINTENANCE OF A THREE-MIRROR ANASTIGMAT USING FULL-FIELD PHASE RETRIEVAL

KEVIN Z. DERBY, JAREN N. ASHCRAFT, PIERRE NICOLAS, SANCHIT SABHLOK, KYLE VAN GORKOM, HYUKMO KANG, DOUG KELLY, PATRICK INGRAHAM, HEEJOO CHOI, DAEWOOK KIM, EWAN DOUGLAS

THE UNIVERSITY OF ARIZONA
COLLEGE OF SCIENCE
STEWARD OBSERVATORY

UASAL LOFT

PHASE RETRIEVAL (PR)

Image-based wavefront sensing method that uses point spread function (PSF) intensity measurements to recover the wavefront phase.

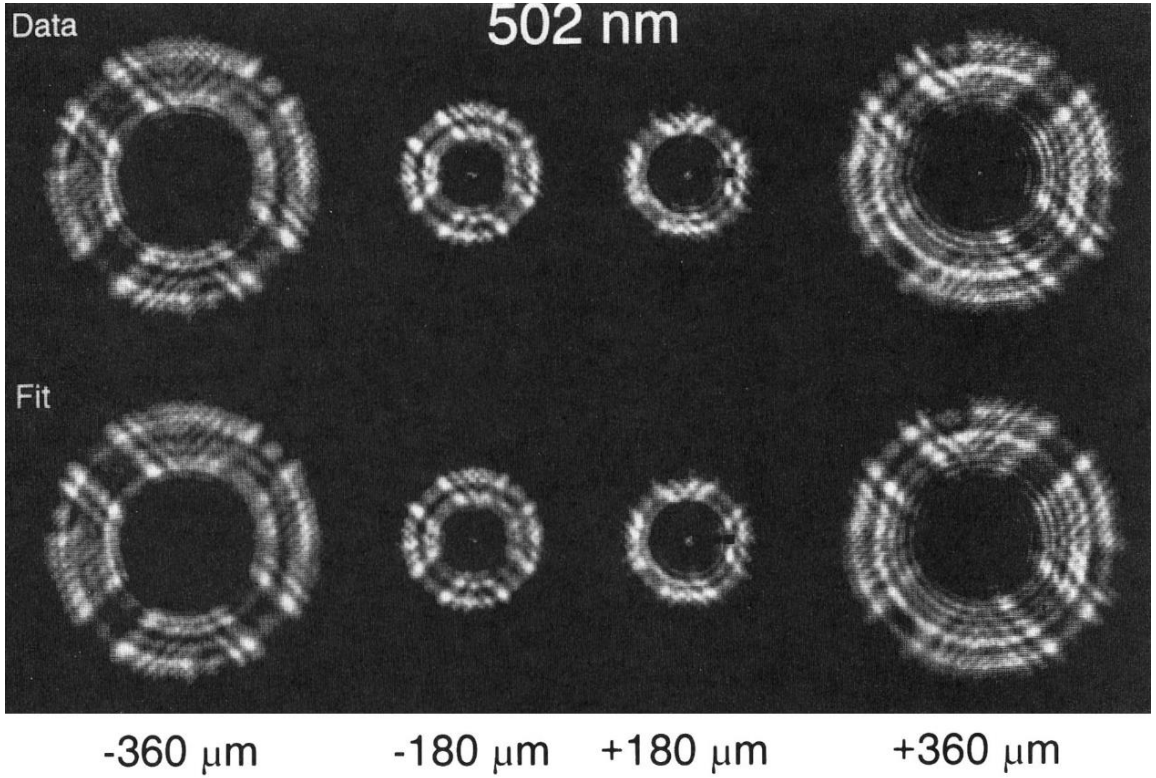

Phase retrieval measurements using WFPC2 on Hubble [2].

Extensive history and use for space telescopes.

- Diagnosed Hubble's primary mirror shape error.
- Used during commissioning of JWST.
- Planned wavefront sensor for Roman Space Telescope.

[2] Krist and Burrows, 1995

PHASE RETRIEVAL (PR)

Image-based wavefront sensing method that uses point spread function (PSF) intensity measurements to recover the wavefront phase.

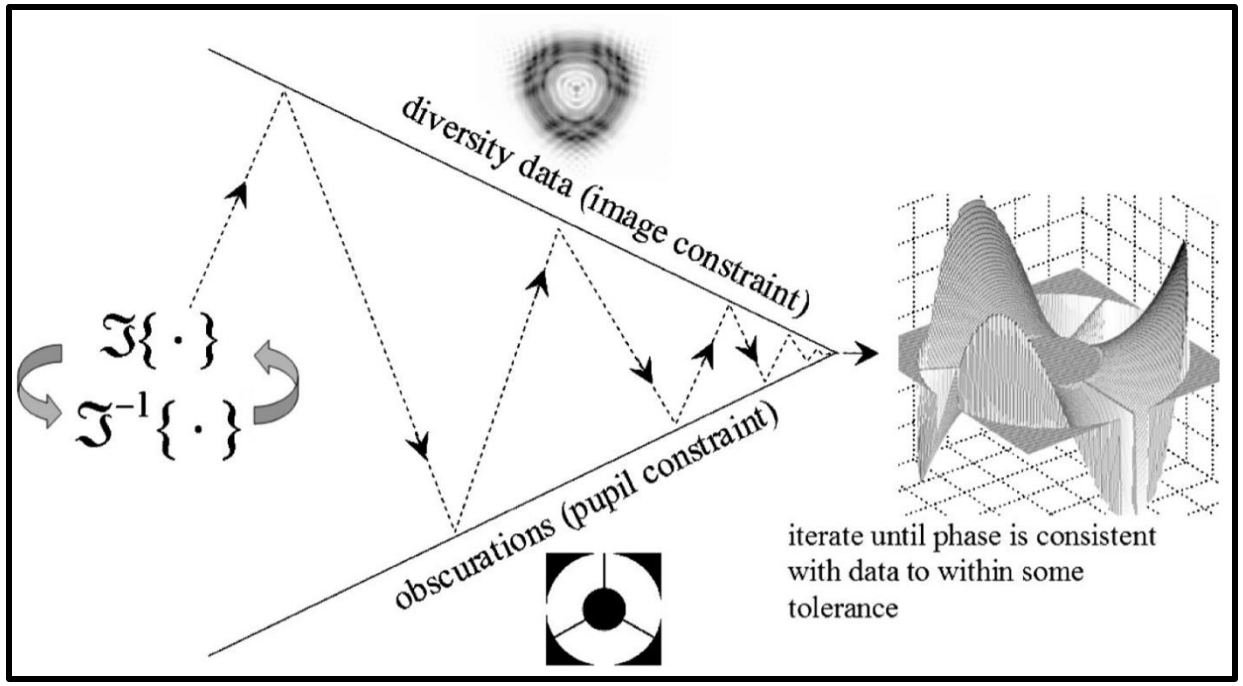

Diagram showing how iterative transform PR converges on a phase estimate [3].

Iterative-transform PR estimates phase by enforcing image and pupil constraints in conjugate Fourier domains.

Simple to implement but has limitations:

- Phase wrapping for multi-wave phase errors.
- Difficult to account for real-world effects.

[3] Dean and Bowers, 2003

PHASE RETRIEVAL (PR)

Image-based wavefront sensing method that uses point spread function (PSF) intensity measurements to recover the wavefront phase.

Table 1. Gradient Rules

Name	Forward Model	Gradient Model	Parameter Domains	#
Addition	$z = x + y$	$\bar{x} = \bar{z},\ \bar{y} = \bar{z}$	$x, y, z \in \mathbb{C}^N$	(47)
Scalar–vector addition	$z = x + y$	$\bar{x} = \sum_n \bar{z}_n,\ \bar{y} = \bar{z}$	$z, y \in \mathbb{C}^N,\ x \in \mathbb{C}^1$	(48)
Element-wise product	$z = x \circ y$	$\bar{x} = y^* \circ \bar{z},\ \bar{y} = x^* \circ \bar{z}$	$x, y, z \in \mathbb{C}^N$	(49)
Matrix product	$z = x * y$	$\bar{x} = \bar{z} * y^{T*},\ \bar{y} = x^{T*} * \bar{z}$	$x \in \mathbb{C}^{N\times P},\ y \in \mathbb{C}^{P\times M},\ z \in \mathbb{C}^{N\times M}$	(50)
Scalar–vector product	$z = xy$	$\bar{x} = \sum_n y_n^* \bar{z}_n,\ \bar{y} = x^* \bar{z}$	$z, y \in \mathbb{C}^N,\ x \in \mathbb{C}^1$	(51)
Raising to a constant power	$y = x^c$	$\bar{x} = c \circ (x^*)^{c-1} \circ \bar{y}$	$x, y \in \mathbb{C}^N,\ c \in \mathbb{R}^N$	(52)
Element-wise square magnitude	$y = \lvert x\rvert^2$	$\bar{x} = 2x \circ \Re\{\bar{y}\}$	$x \in \mathbb{C}^N,\ y \in \mathbb{R}^N$	(53)
Real part	$y = \Re\{x\}$	$\Re\{\bar{x}\} = \Re\{\bar{y}\}$	$x \in \mathbb{C}^N,\ y \in \mathbb{R}^N$	(54)
Imaginary part	$y = \Im\{x\}$	$\Im\{\bar{x}\} = \Re\{\bar{y}\}$	$x \in \mathbb{C}^N,\ y \in \mathbb{R}^N$	(55)
Complex exponential	$y = e^x$	$\bar{x} = \bar{y} \circ y^*$	$x, y \in \mathbb{C}^N$	(56)
Imaginary complex exponential	$y = e^{ix}$	$\bar{x} = \Im\{\bar{y} \circ y^*\}$	$x \in \mathbb{R}^N,\ y \in \mathbb{C}^N$	(57)
Basis function expansion	$y = \sum_n a_n \boldsymbol{B_n}$	$\bar{a}_n = \sum_{u,v} \bar{y}_{u,v} B_n(u, v)$	$y \in \mathbb{R}^{N\times M},\ \boldsymbol{B} \in \mathbb{R}^{P\times N\times M},\ \boldsymbol{a} \in \mathbb{R}^P$	(58)
Array indexing	$y = x[\![\alpha]\!]$	$\bar{x}[\![\alpha]\!] = \bar{y}$	$x, y \in \mathbb{C}^N,\ \alpha$ is an index	(59)
Array assignment	$y[\![\alpha]\!] = x$	$\bar{x} = \bar{y}[\![\alpha]\!]$	$x, y \in \mathbb{C}^N,\ \alpha$ is an index	(60)
Scalar broadcasting	$y_n = x,\quad \forall\ n$	$\bar{x} = \sum_n \bar{y}_n$	$y \in \mathbb{C}^N,\ x \in \mathbb{C}^1$	(61)

Gradient backpropagation rules used for creating reverse models [5].

Parametric PR estimates phase by fitting model parameters to empirical data.

Better performing nonlinear optimization algorithms require access to the gradient.

- Analytical derivation using math.
- Automatic differentiation (autodiff) using a package like JAX [4].
- Algorithmic differentiation (algodiff) using gradient rules [5] and a numerical optics package which supports reverse modeling like prysm [6].

[4] github.com/jax-ml/jax
[5] Jurling and Fienup, 2014
[6] github.com/brandondube/prysm

PHASE DIVERSITY

When performing PR, we need to modulate the PSF with a known diversity function.

-2λ Defocus

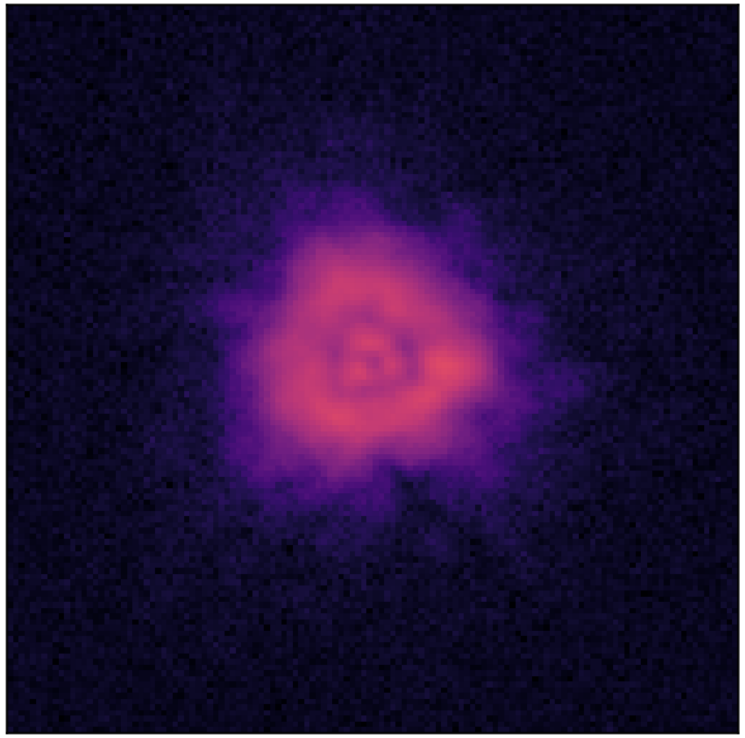

0λ Defocus

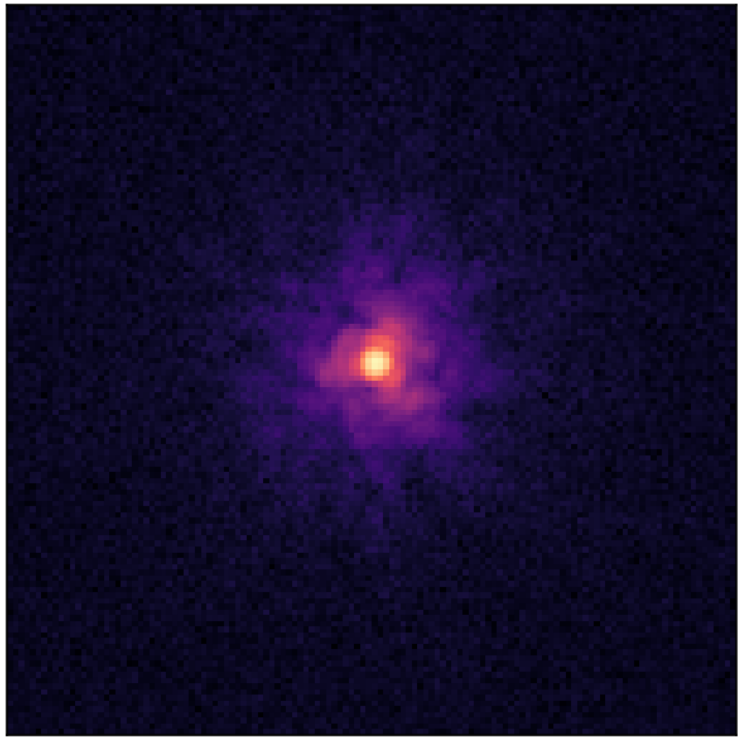

+2λ Defocus

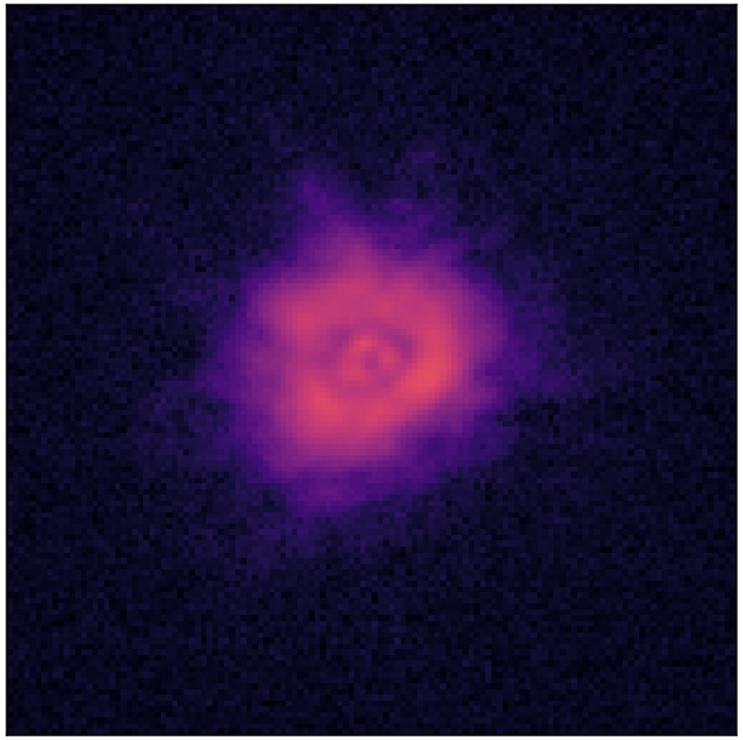

Defocus is commonly used as the diversity function because it is easy to implement and spreads energy equally.

PHASE DIVERSITY

When performing PR, we need to modulate the PSF with a known diversity function.

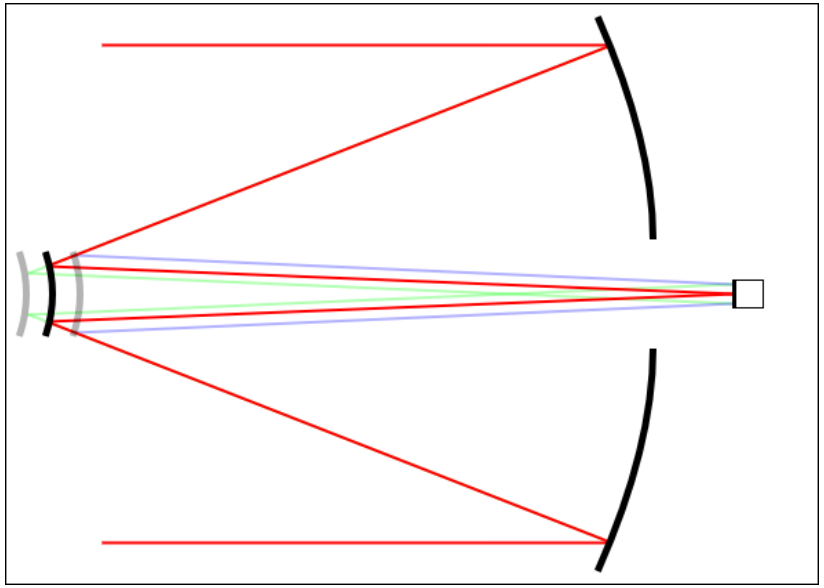

Pistoning the secondary mirror gives defocus but also introduces other aberrations.

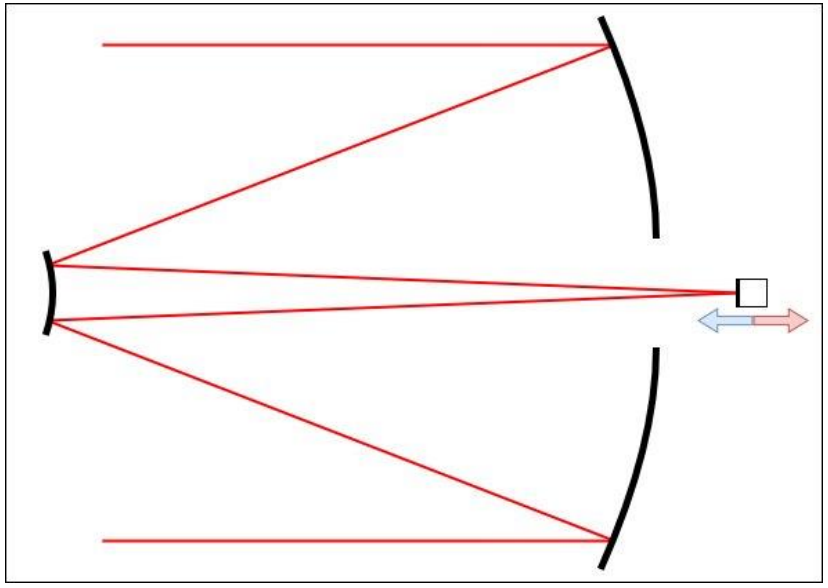

Axially shifting the detector gives defocus but introduces more moving parts.

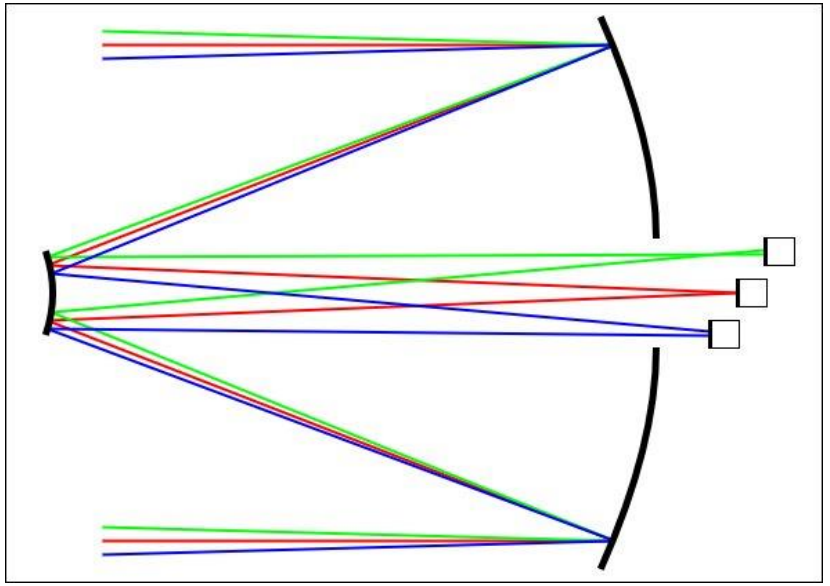

If multiple detectors are used to tile the FOV, we could axially shift several of them to give defocus.

THREE MIRROR ANASTIGMAT (TMA)

Uses 3 mirrors to minimize coma, astigmatism, and spherical aberrations across a large FOV. The James Webb and Roman space telescopes both utilize this design philosophy.

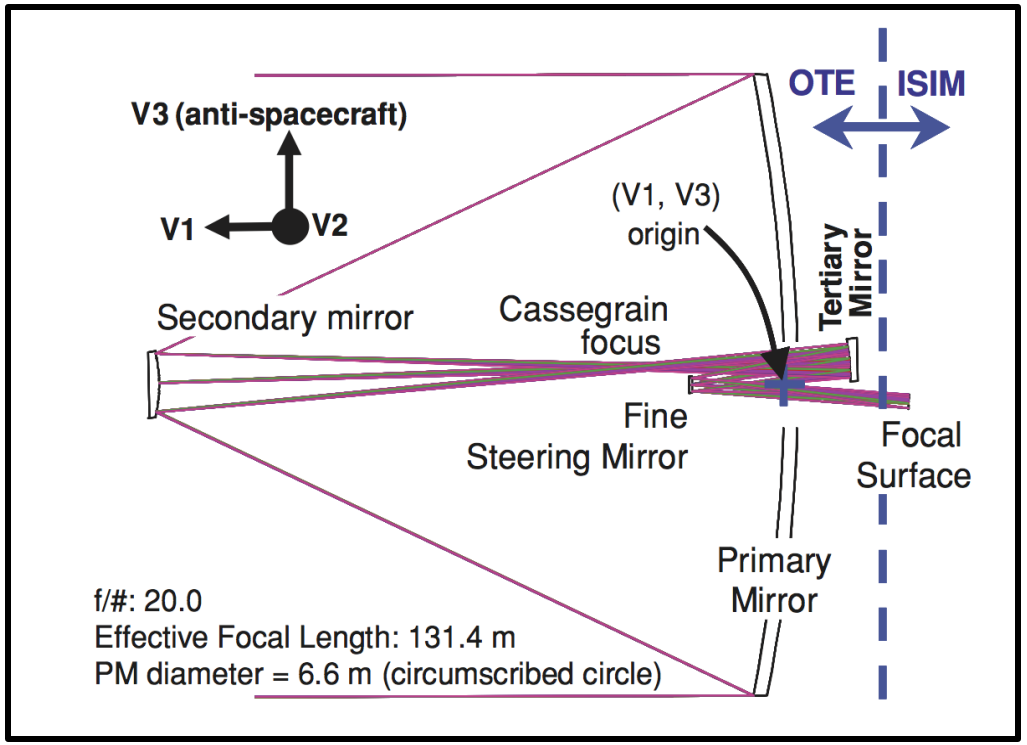

The James Webb Space Telescope optical design [7].

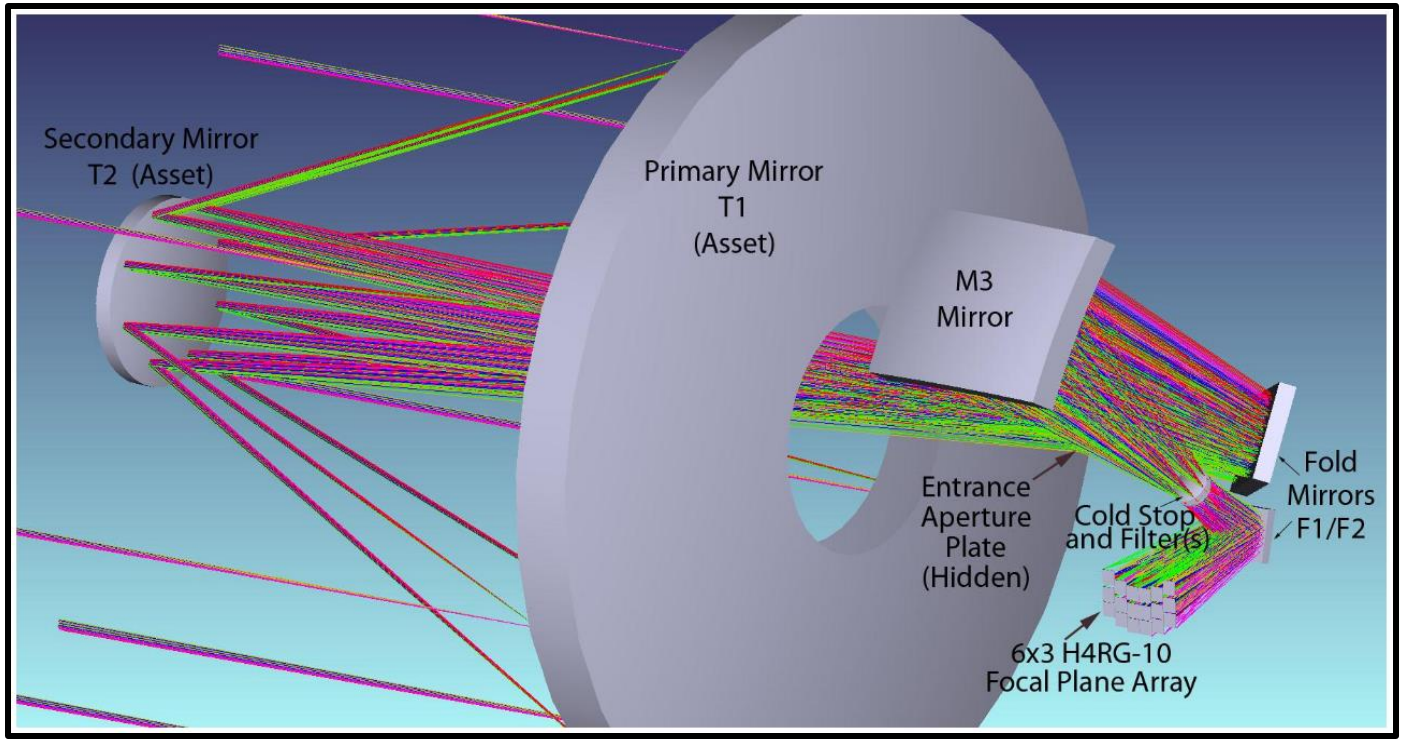

The Roman Space Telescope Optical Design [8].

[7] Gadner et al. 2003
[8] Pasquale et al. 2014

3-METER OFF-AXIS TMA DESIGN

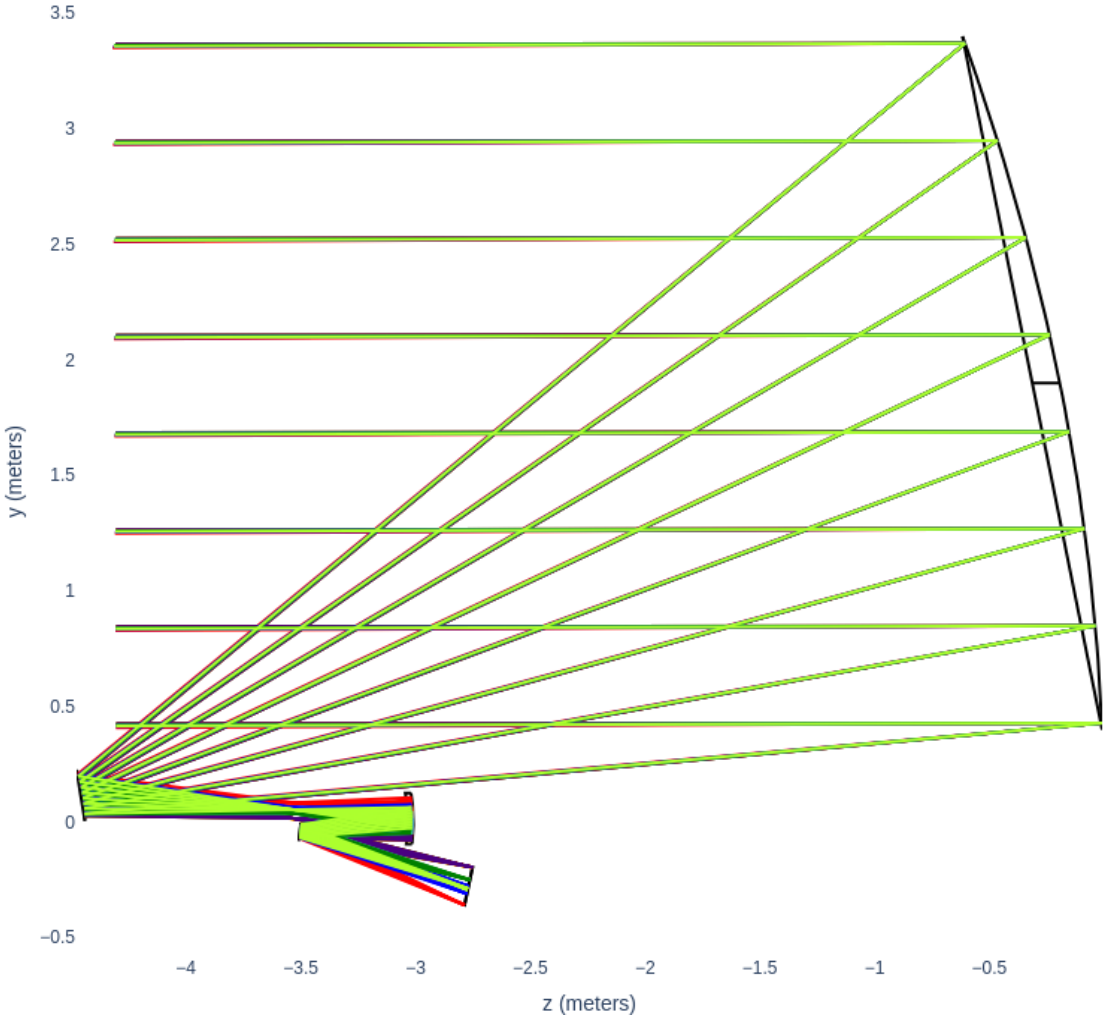

Parameter	Value
Central Wavelength	625 nm
Bandwidth	24%
Working F/#	14.06
Effective Focal Length	42046 mm
Platescale	4.905 arcsec/mm

Optical layout and key parameters for a 3-meter off-axis TMA design as described by Kim et al. 2025.

3-METER OFF-AXIS TMA DESIGN

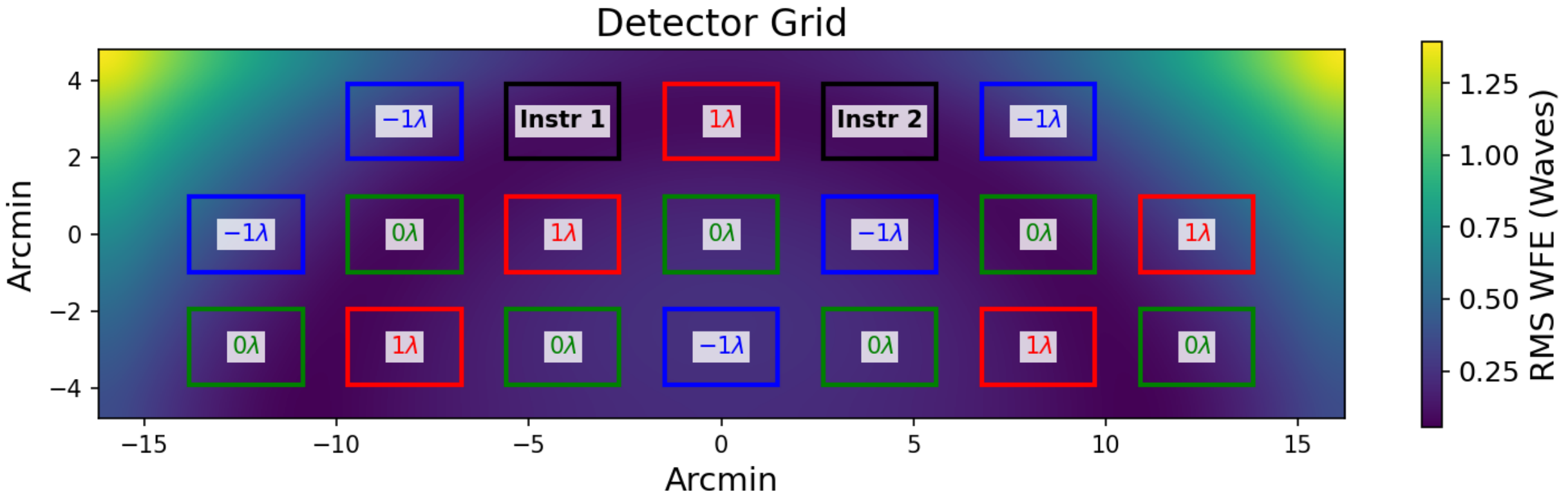

The large FOV requires many detectors. We assume a checkered grid of in-focus and out-of-focus detectors giving us focus diversity for PR so long as an adequately bright star falls on it.

FIELD DEPENDENT ABERRATIONS

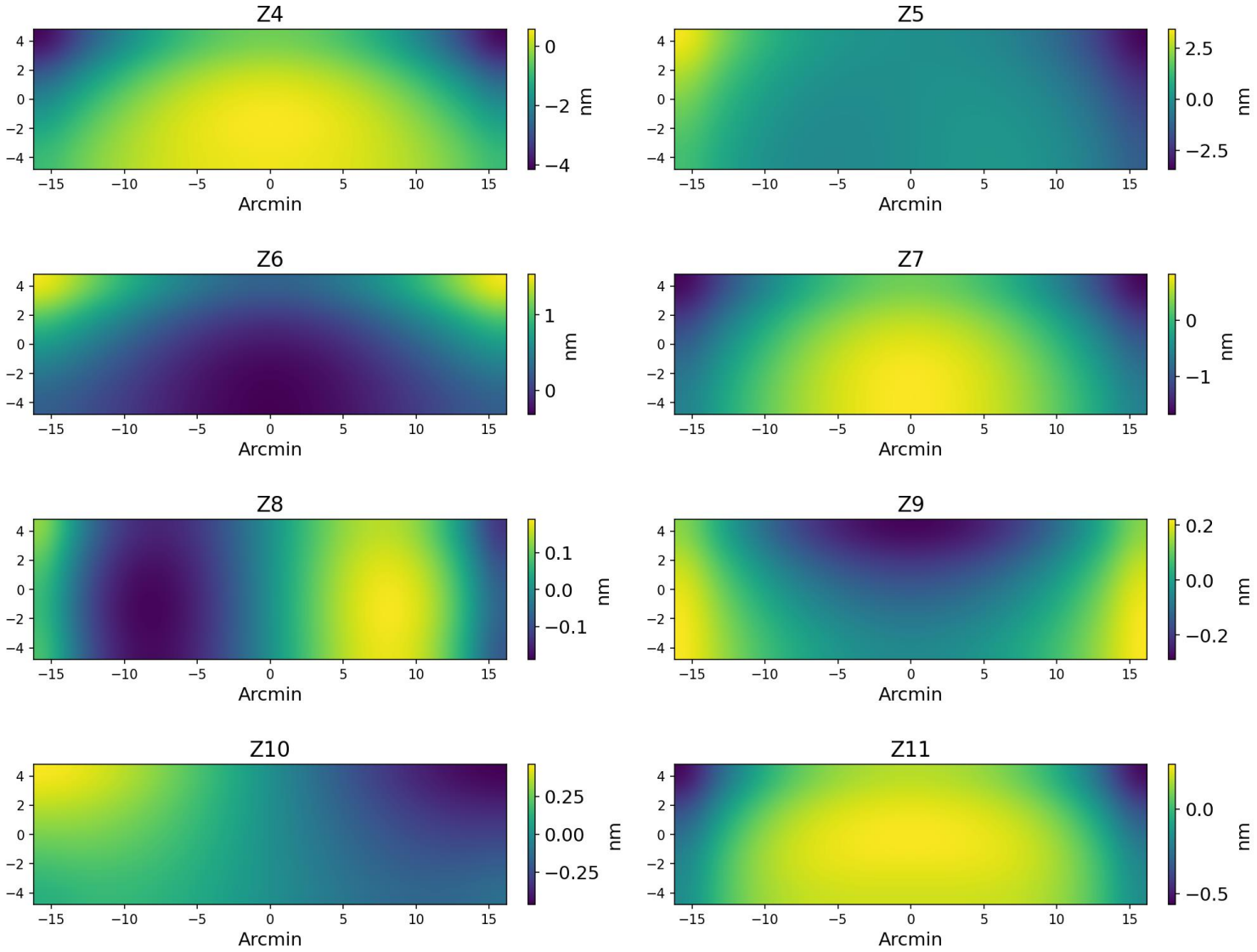

Field dependent aberrations at nominal alignment show nonlinear variations across the field.

Misalignments result in linearly varying deviations from this nominal state [9].

[9] Thompson et al. 2008

FIELD DEPENDENT ABERRATIONS

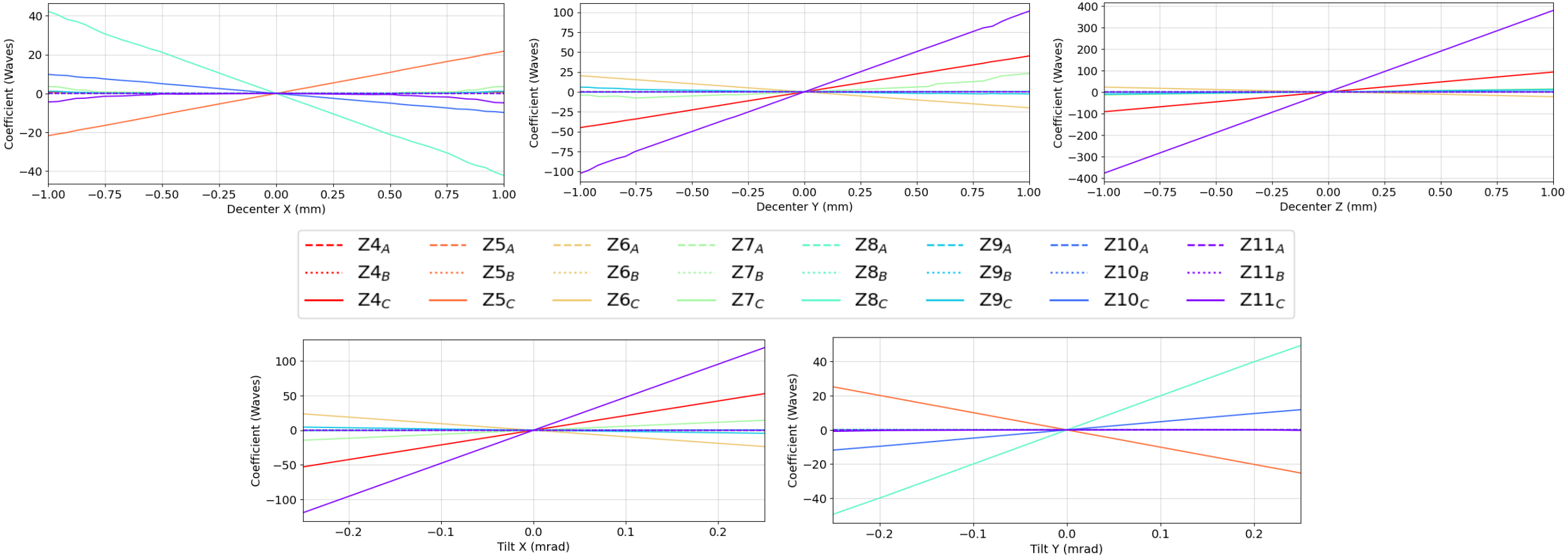

Misaligning M1 causes linearly varying deviations from field dependent aberrations at nominal alignment.

FIELD DEPENDENT ABERRATIONS

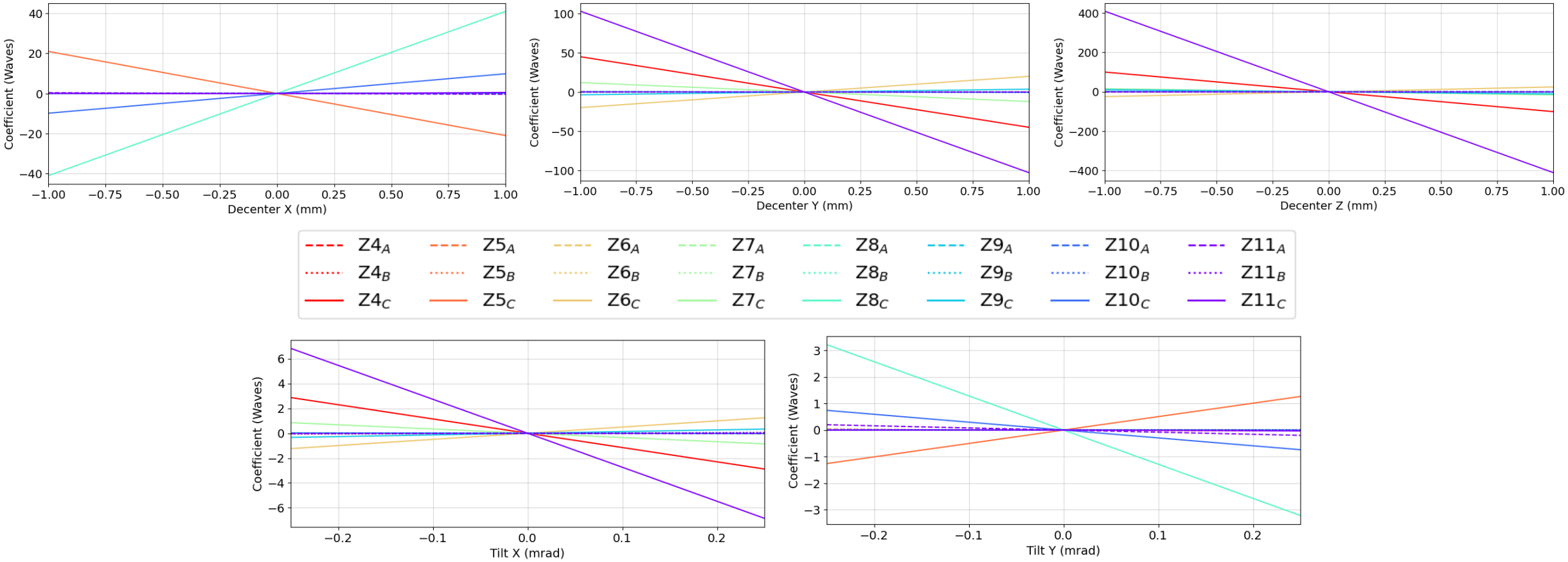

Misaligning M2 also causes linearly varying deviations from field dependent aberrations at nominal alignment.

FULL-FIELD PR (FFPR)

1. We have a TMA design giving us a large FOV...

2. We have a linear model for calculating field-dependent aberrations...

3. We have a checkered grid of in and out-of-focus detectors giving us defocus diversity...

We have all the ingredients to create a parametric PR algorithm which can estimate the wavefront across the FOV in a single shot!

FFPR EXAMPLE: SIMULATED PSFS

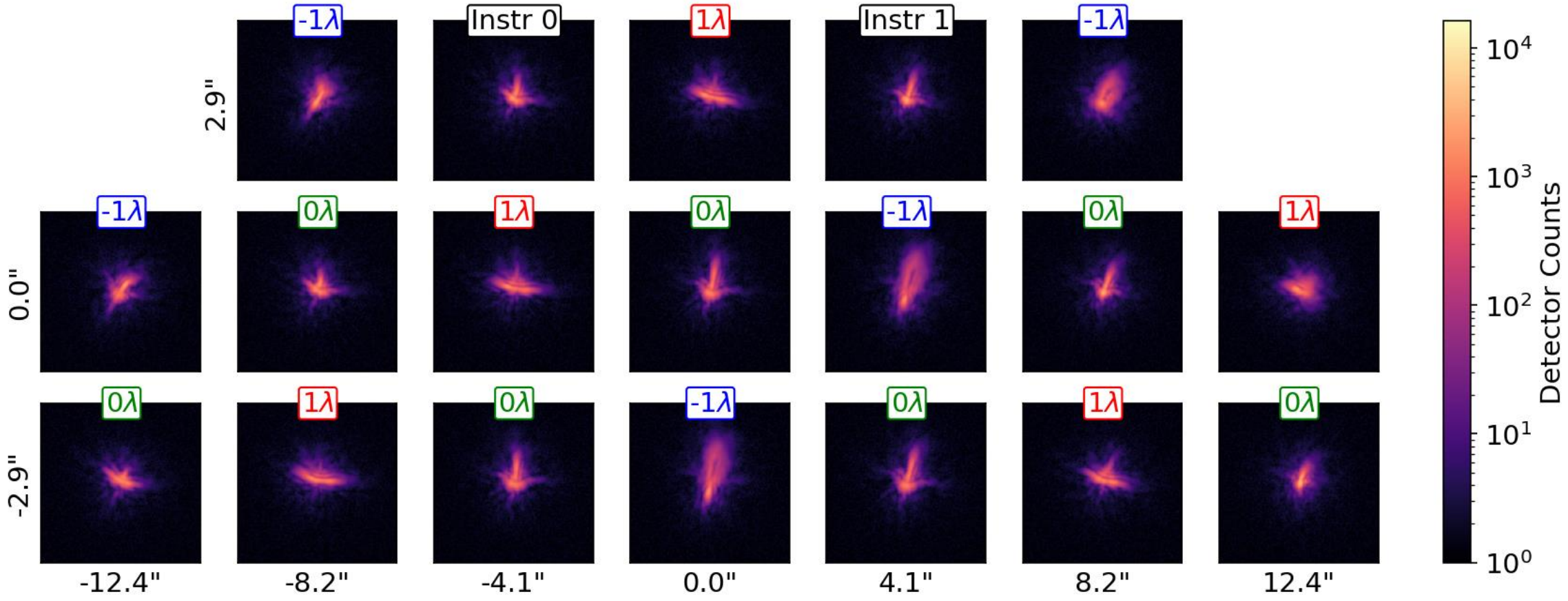

Simulated PSFs for FFPR. Fields points are given to a raytrace model which outputs field-dependent WFE. These are fed to a diffraction + detector model to simulate noisy PSFs.

FFPR EXAMPLE: OPTIMIZATION ROUTINE

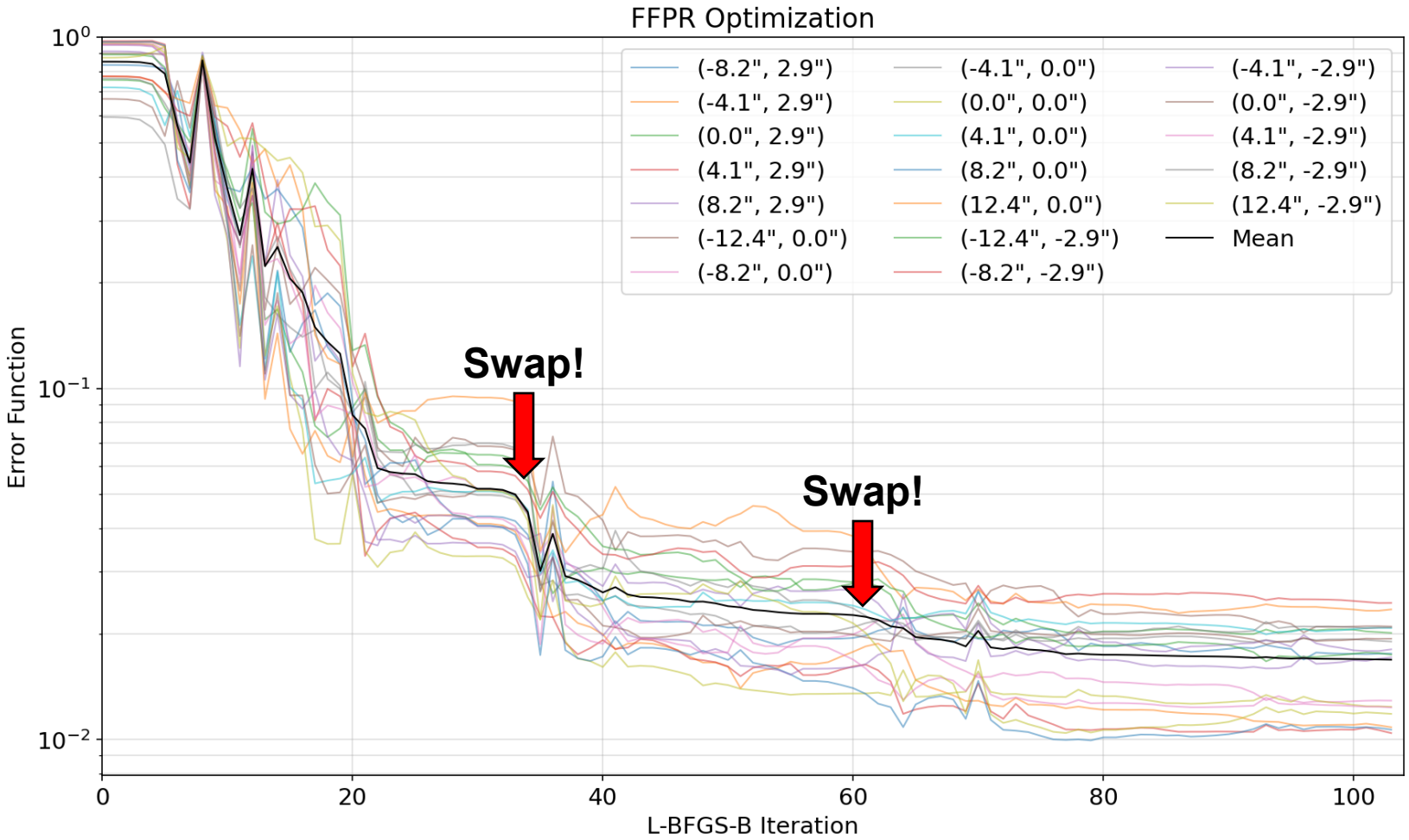

We use L-BFGS-B as our nonlinear search algorithm. We swap between optimizing field-dependent aberrations and common-path aberrations caused by optical surface errors.

FFPR EXAMPLE: ESTIMATED WFE

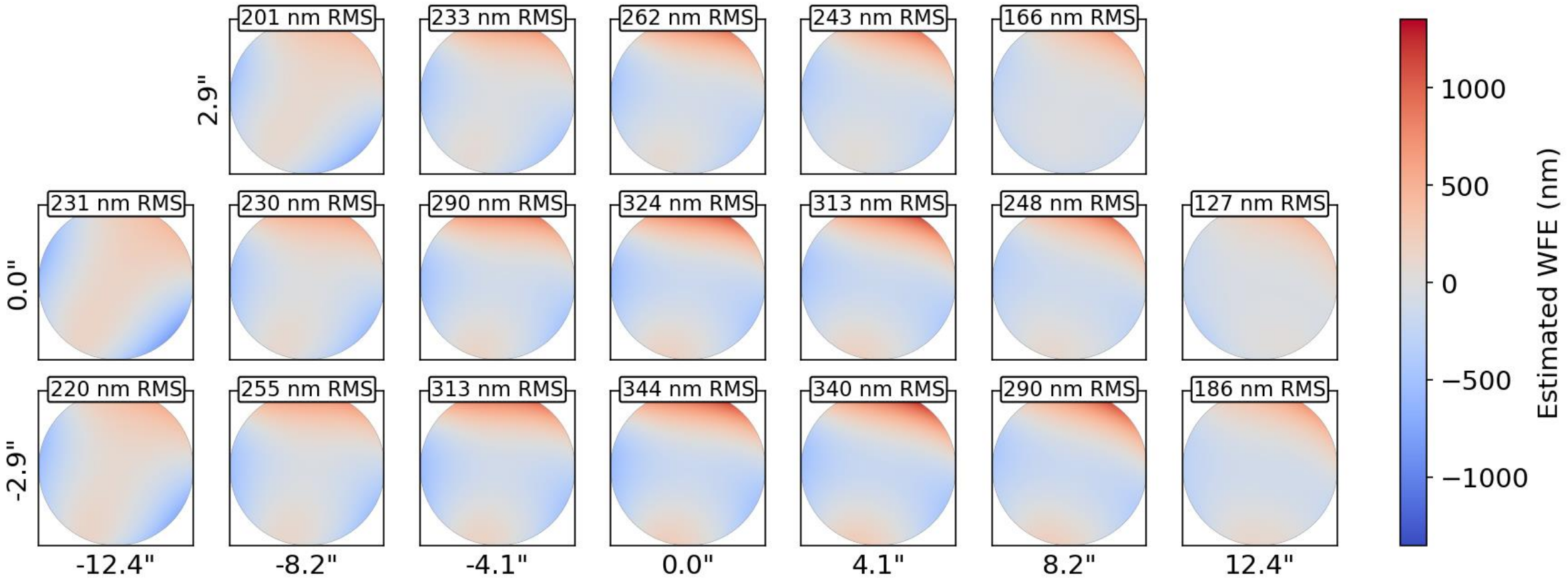

Estimated WFE for the PSFs shown previously. We can recover multi-wave phase errors across the FOV in a 24% bandpass.

FFPR EXAMPLE: ESTIMATE RESIDUALS

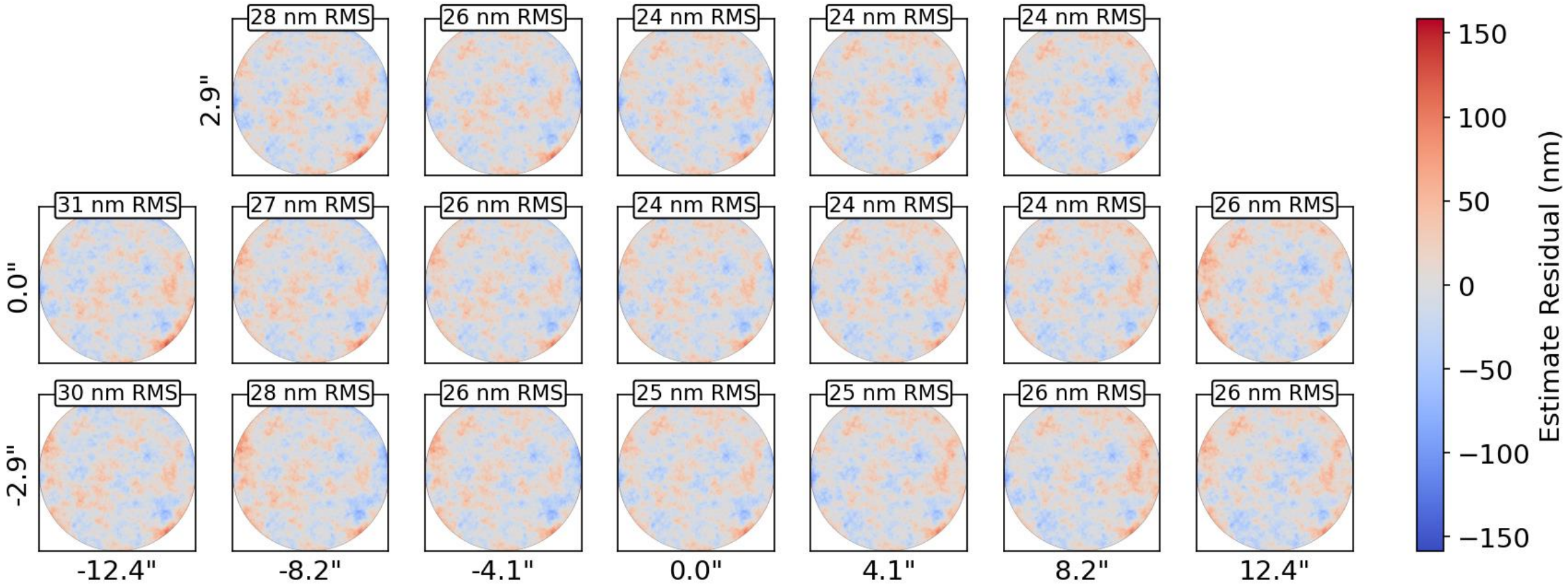

Estimate residuals for the estimated WFEs shown previously. Since we only estimate up to Z37, the residuals correspond to higher-order optical surface errors present in our system.

ALIGNMENT SIMULATION

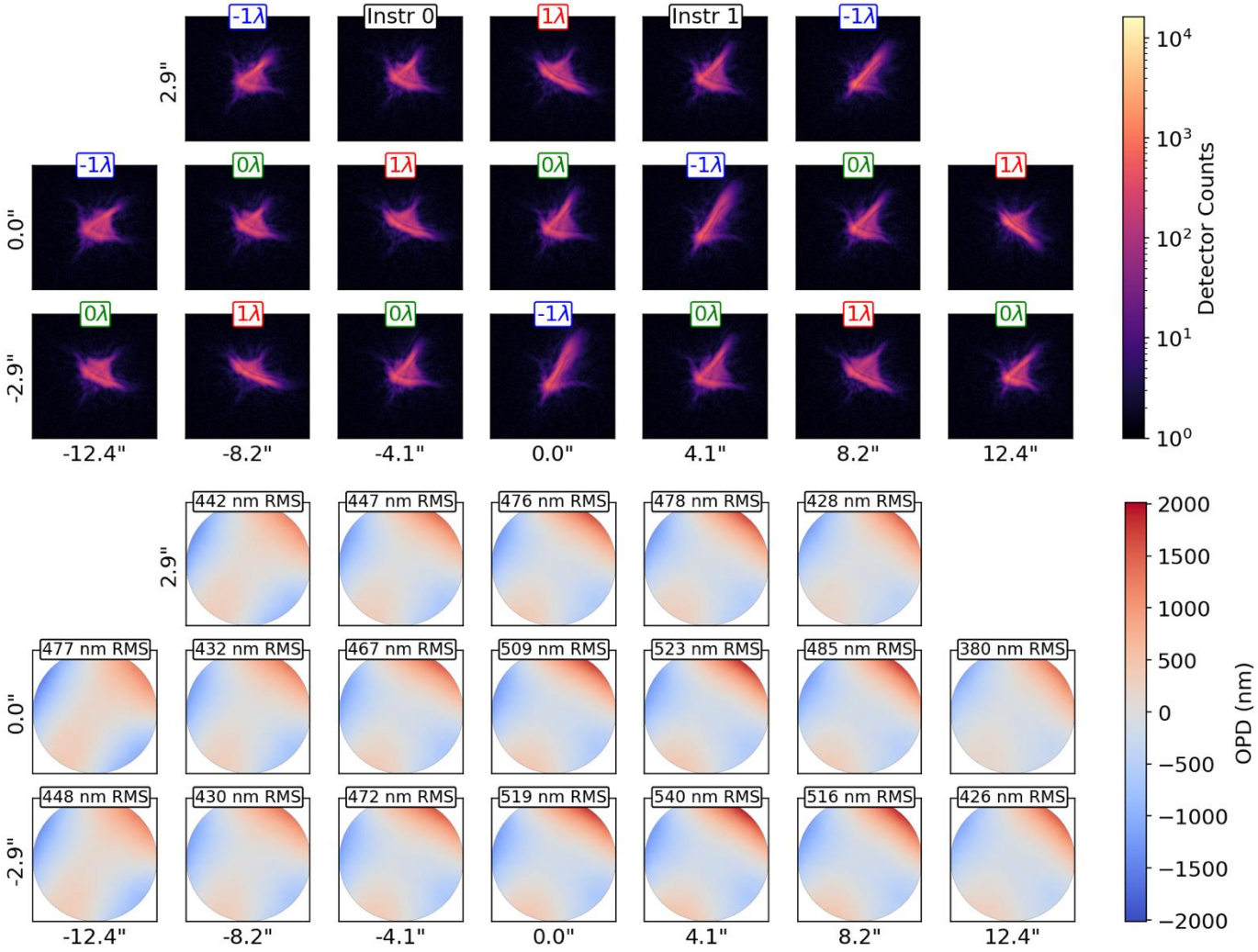

See Solvay's Talk at 11 AM in Room 6C to see where these come from!

M1 Misalignment	Value
Decenter X	-286 µm
Decenter Y	67 µm
Decenter Z	-162 µm
Tilt X	6 µrad
Tilt Y	-21 µrad
M2 Misalignment	**Value**
Decenter X	-311 µm
Decenter Y	44 µm
Decenter Z	-139 µm
Tilt X	73 µrad
Tilt Y	-81 µrad

We assume a set of initial misalignments which result in ~6 waves of peak-to-valley wavefront error across the FOV after coarse alignment.

ALIGNMENT SIMULATION

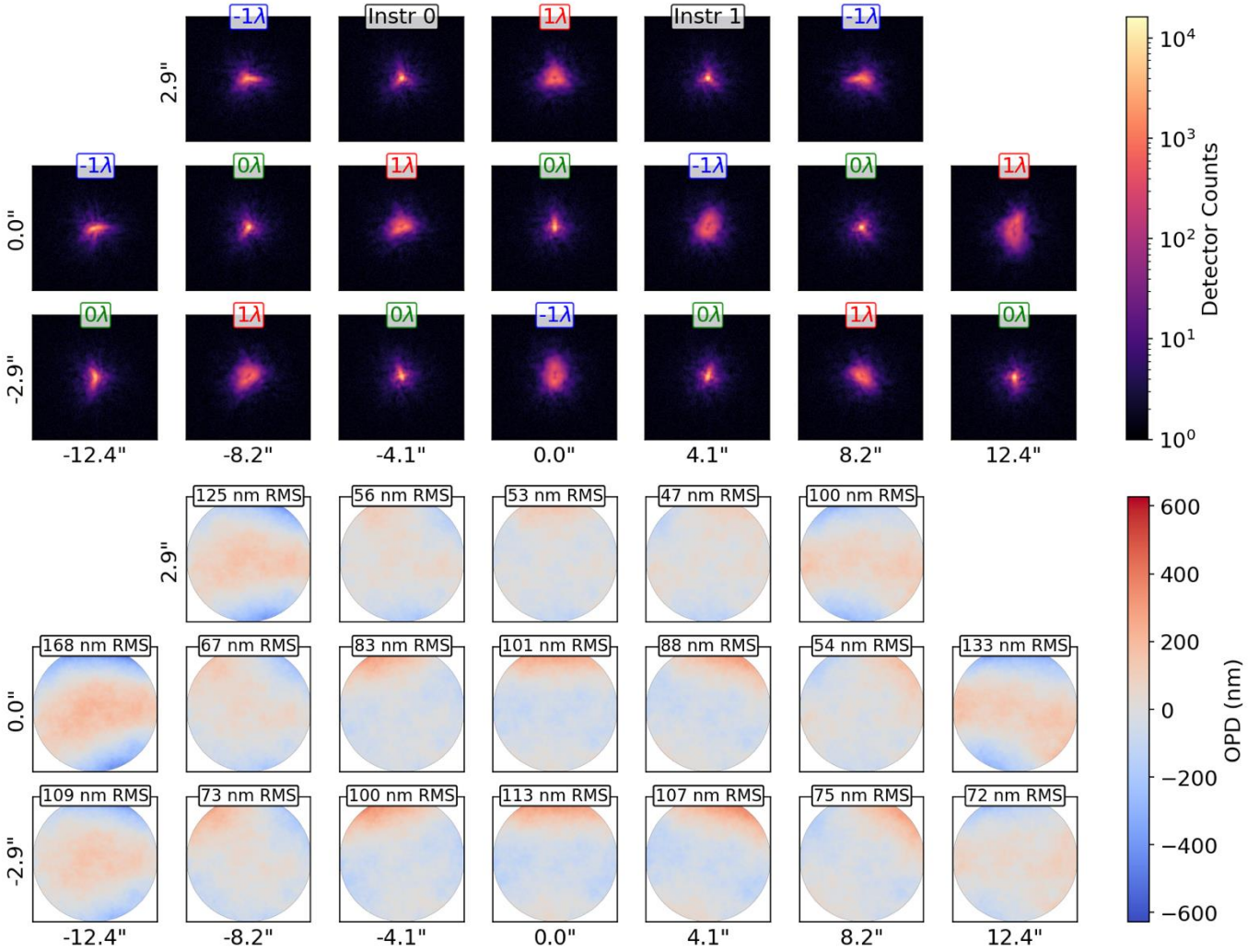

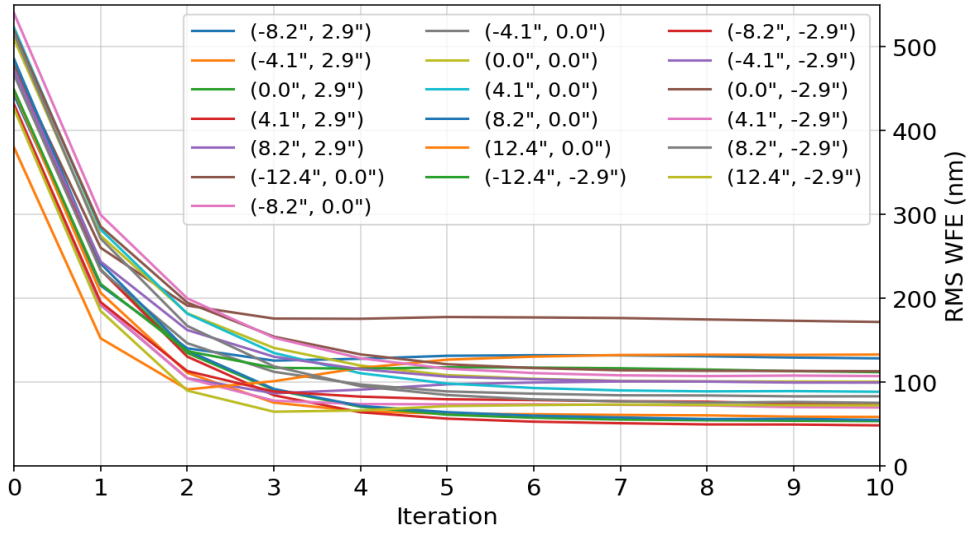

We can bring the telescope into alignment with 10 iterations of closed-loop FFPR with M1 + M2 bulk motion corrections. Both instrument fields achieve >0.8 Strehl.

MAINTENANCE SIMULATION

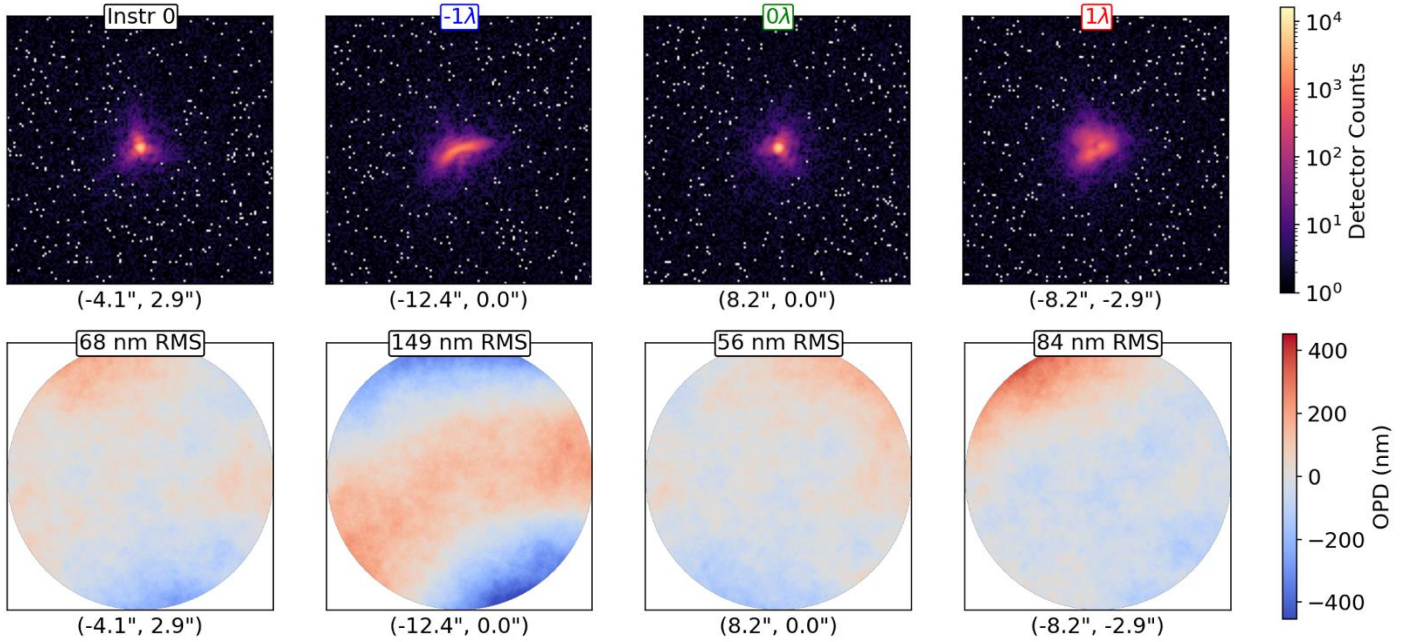

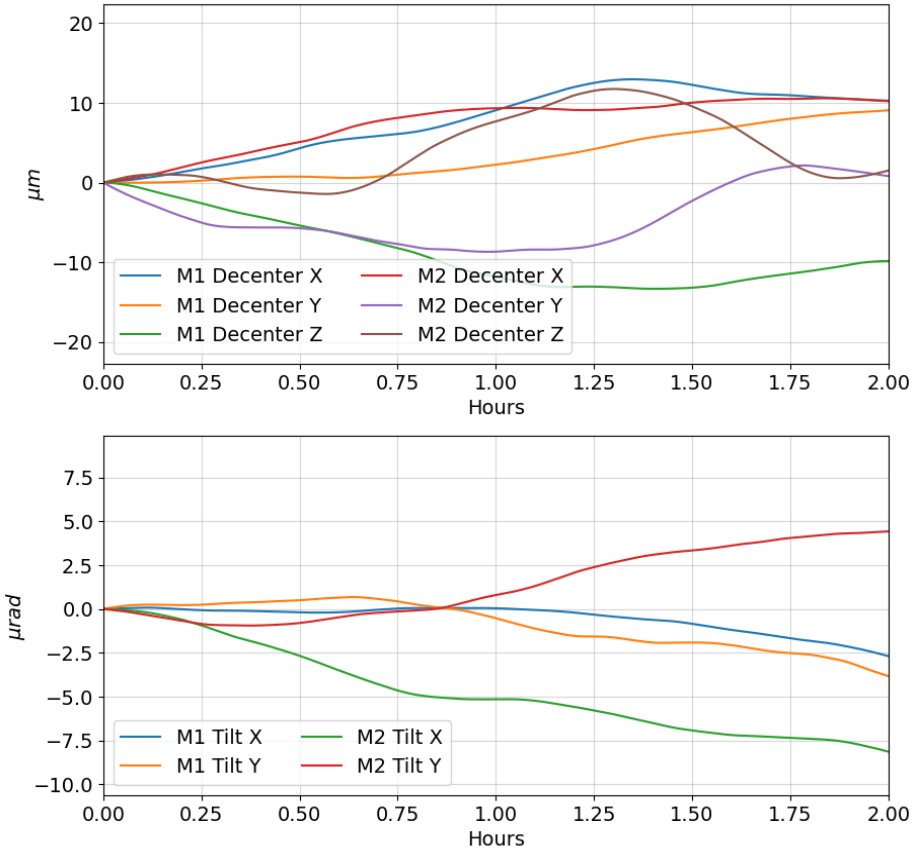

Timeseries of M1 + M2 misalignments were generated using power spectra. We assume only a few dim guide stars to guide closed-loop FFPR during science observations.

MAINTENANCE SIMULATION

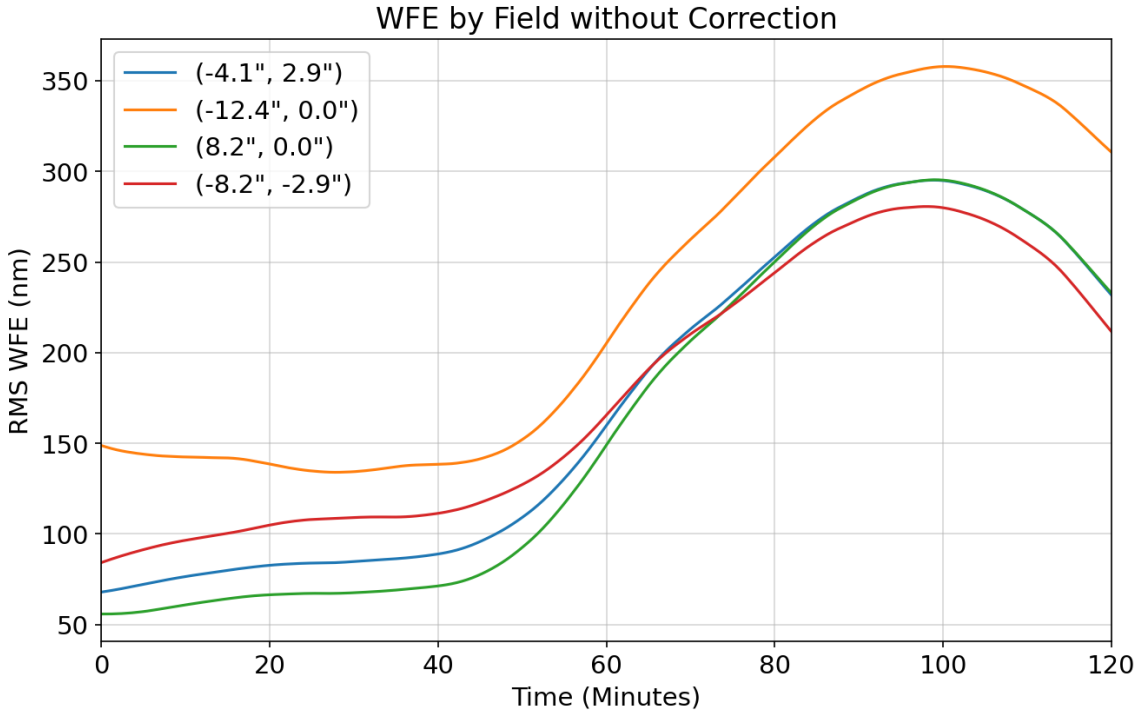

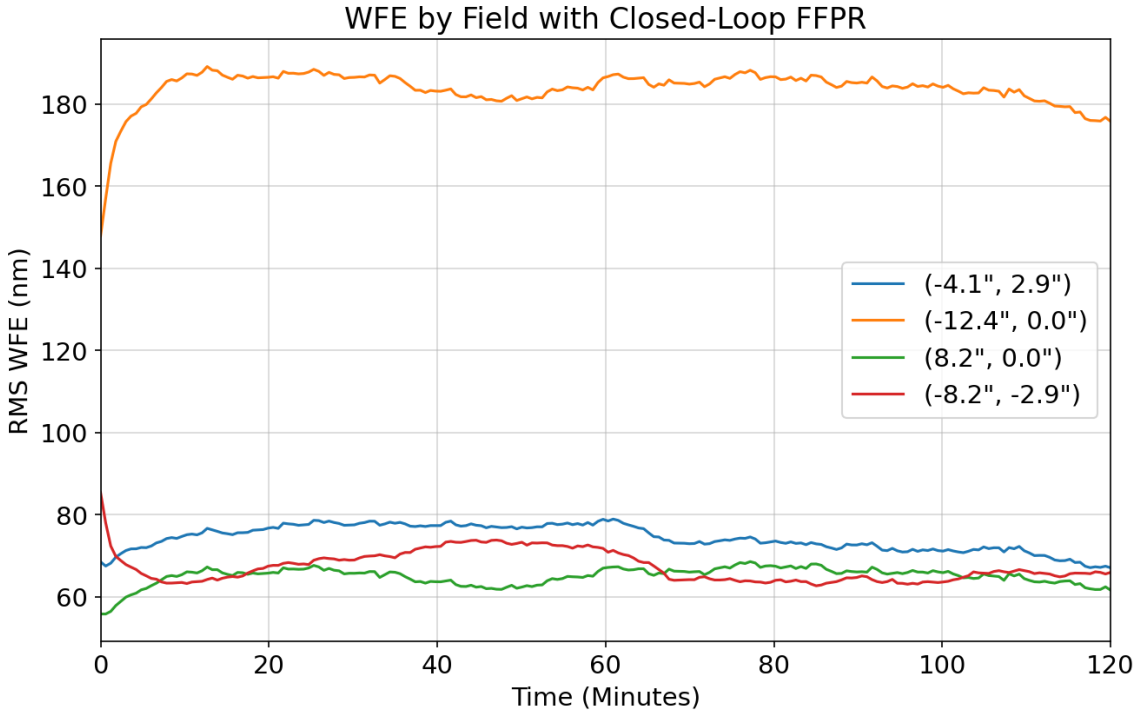

WFE by field with and without closed-loop FFPR. The instrument field is located at (-4.1", 2.9") and stays within the range of 70 – 80 nm RMS.

CONCLUSION

- We have developed a parametric, full-field phase retrieval algorithm capable of estimating aberrations across the FOV of a wide-FOV telescope using a checkered grid of in and out-of-focus detectors.
- We have demonstrated the feasibility of aligning the telescope using our algorithm for wavefront sensing.
- We have demonstrated the feasibility of maintaining a stable telescope wavefront at the nanometer level using our algorithm for wavefront sensing.

Future work

- Examine guide star requirements for telescope alignment and wavefront maintenance.
- Add the field-dependent pupil to the telescope model for simulating PSFs and account for this in our FFPR algorithm.
- Explore the ability to perform full-field phase retrieval without the use of out-of-focus detectors.

ACKNOWLEDGEMENTS

Portions of this research were supported by funding from the Technology Research Initiative Fund (TRIF) of the Arizona Board of Regents and by generous anonymous philanthropic donations to the Steward Observatory of the College of Science at the University of Arizona.

THANK YOU

Contact: derbyk@arizona.edu

Code: github.com/zhangderby/ffpr

THE UNIVERSITY OF ARIZONA
COLLEGE OF SCIENCE
STEWARD OBSERVATORY

UASAL LOFT